MEASUREMENT AND ANALYSIS OF VIBRATIONAL BEHAVIOUR OF AN SNR–FUEL ELEMENT IN SODIUM FLOW

B.F.H. HEß, E. RUPPERT, H. SCHMIDT, K. VINZENS

INTERATOM, Internationale Atomreaktorbau GmbH, D-506 Bensberg/Köln, Germany

SUMMARY

Within the framework of SNR-300 fuel element development programme a complete full size fuel element dummy has been tested thoroughly for nearly 3000 hours at 650°C system temperature in the AKB sodium loop at Interatom, Bensberg. Investigations of the hydraulic characteristics by measurement of specific pressure losses, flow velocities, leakage flow through the piston rings and investigations of its vibrational behaviour were part of this endurance test at elevated temperatures. The pressure drop versus flow and the leakage measurement are mentioned briefly to confirm the correctness of the test hydraulics. The vibrational behaviour of the element and the approach to analysis is the main object of this report.

It is known that the coolant flow through a subassembly can induce flutter or vibrations of structural parts such as single pins, the wrapper and the total pin bundle all of which have been of interest during this test. To detect these vibrations of different structural parts simultaneously with a minimum of instrumentation only 3 weldable high temperature strain gauges were employed. These strain gauges were especially prepared and bent in such a way as to form a bridge between the inner wrapper and a fuel pin top and spot-welded to both the wrapper and the fuel pin. Although this arrangement seems to be a rather unusual one, the simultaneous measurement of bundle, wrapper and pin vibrations was possible and periodic flow fluctuations were also detected.

This is clearly reflected by the power spectral densities of the analysed signals which are rather complex and difficult to interpret. A simplified empirical approach has therefore been adopted describing the integral vibrational behaviour of complex structures like core elements in terms of experimental response functions over the flow range of technological interest. These response functions could be interpreted qualitatively as the vibration to flow response and clearly indicate resonances for flow induced vibrations at certain flow rates. This simple approach to vibration analysis seems especially suitable for measurements in sodium flow, which should however be considered as technologic supplement to the fundamental studies conducted in water or air.

The presented results are only relative due to calibration difficulties with these deformed strain gauges which were first used during this test. It is, however, believed that this arrangement, in connection with the proposed analytical approach, leads to a simple and technical representation of the vibrational behaviour of core elements during sodium tests. Detailed information needed for check and calibration of computer codes are however displayed by the respective power spectral density functions.

1. Introduction

During the years of reactor operation it has been realized that coolant flow represents a form of statistically fluctuating energy which can induce various mechanisms as for instance cavitation and vibration. Induced vibrations of structural parts enhance fatigue and wear leading to anomalous reactor performance or even to failure, as experience has shown.

Much effort has therefore been devoted by numerous investigators to understand these phenomena, first, to learn the causes of local pressure fluctuations as well as the vibration response of structural parts and then to design in such a way as to reduce the response of critical components. Almost all investigations have been conducted in water or gas loops using rather idealized experimental arrangements. The results were adopted for a design guide, with appropriate modifications also for components of the Liquid Metal Fast Breeder Reactor (LMFBR). It is admitted that this approach leads to a better and increasing insight into fundamentals of flow-induced vibrations but will not eliminate full-scale tests of critical LMFBR-components.

Such tests mainly considered as endurance tests to demonstrate integrity can simultaneously be used to ascertain the predicted vibrational behaviour of the component tested. Due to the not-fully developed state of art in sodium instrumentation and the fact that the tested structures are not at all idealized arrangements but rather complex reactor components the experimental approach, analysis and interpretation of results differ from those applied during water tests in several aspects. It is the aim of this report to demonstrate how an endurance test of a complete subassembly in sodium can give a simple technological picture of its vibrational behaviour, ascertaining the feasibility of subassembly design with respect to flow-induced vibrations.

2. Subassembly and instrumentation

As part of the research and development program of the SNR (schneller natriumgekühlter Reaktor) a complete, full-size fuel subassembly dummy was tested for nearly 300 hours at 650°C in the AKB-sodium loop at Interatom. The subassembly shown schematically in fig. 1 consisted of 166 fuel pin dummies, filled with silver pellets for fuel density simulation and 3 tie rods to which the 14 spacer grids were fixed. This fuel pin bundle was free-standing inside a hexagonal wrapper and supported only by the anchor grid plate, fixed to the wrapper and into which the pins were screwed with a given torque. Along its axis the fuel pin bundle was centered in the wrapper by means of springs which were attached to the outer surfaces of the spacer grids as shown in fig. 1.

The nominal gap between wrapper and spacer grid (without spring) amounted to 0.4 mm, allowing free vibration, damped by the springs in case of ideal symmetry.
Three weldable, high temperature strain gauges were used as vibration sensors. These strain gauges were especially prepared and bent in such a way as to form a bridge between the wrapper and a fuel pin top, spot-welded to both, the wrapper and the fuel pin. This rather unusual arrangement, illustrated in fig. 2, was used for the first time and for this reason was not properly calibrated.
Subassembly coolant flow and leakage flow through the piston rings were measured with eddy current flowmeters (ECF's) [1] and the pressure losses of the total subassembly and across two characteristic bundle sections were monitored to verify normal hydraulic behaviour during the tests.

3. Experimental approach and signal processing

It is known that pressure fluctuations inducing vibrations are partly due to the test loop itself and are characteristic for that special loop. For this reason and the complex nature of expected results, as few as possible parameters (pump speed, gate valves etc.) were changed during the isothermally conducted experiments. The signals were recorded on magnetic tape and analyzed with an off-line computer which determined the power spectral density (PSD) functions by means of a Fast Fourier Analysis employing averaging technique (100 samples) to achieve reliable statistics.

It should be mentioned that during analysis, the well-known coherence and correlation functions between strain gauge signals and between strain gauge and ECF signals have also been computed. Although these functions are very helpful for interpretation of results, it is not referred to explicitely since the proposed simple model is based upon power spectral densities.

4. Analysis of structural vibrations

4.1 General considerations

Due to the experimental arrangement, rather complex PSD-spectra are to be expected, since the strain gauges respond to vibrations of different structures such as the wrapper, the fuel pin bundle and those fuel pins to which they are fixed. Besides those vibrations coolant velocity, fluctuations might be detected due to the fluctuations of dynamic pressure acting on the gauges. Vortex shedding behind the strain gauges can also cause vibrations, which in our case most likely are not detected because of their high frequency.

Assuming a linear system the total signal detected is thus a superposition of the vibrations listed above which could be excited and sensed to a varying extent.

Fig. 3 shows a schematic representation of a typical PSD-function as obtained during analysis and of the calculated proper frequency ranges of structure vibrations as well as the frequency characteristics of signal processing equipment. We shall frequently refer to this scheme during the interpretation of results.

4.2 Modal analysis of the structural parts

Normal modes and proper frequencies of all structural parts involved are required for the analysis and the interpretation of obtained PSD-functions. The modal analysis has been carried out and extended up to 11 modes using a computer code which is based on the numerical method of transfer matrices [2]. Some representative results are given in fig. 4 for information. The validity of the calculations with this computer code has been ascertained by various specific experiments conducted in water.

4.3 Simplified transfer model

Exact analysis of the complex PSD-functions obtained with the described experimental arrangement requires detailed theoretical and experimental investigations and knowledge concerning the system of structures under test. These requirements can not be met during a full-scale endurance test conducted under sodium in large test facilities. Neither are ideal arrangements realized, nor are the boundary conditions and influences upon the system generally known, but they should, however represent a technological average as the most realistic situation. The interpretation of the results derived from such measurements is therefore rather difficult.

Some experimental investigations reported recently [3,4] indicate the possibility of describing the vibrational behaviour of complex structures by means of "selective transfer functions". As will be discussed, these functions establish an empirical relationship between both - the RMS-values of strain and of pressure fluctuations as acting force in appropriately selected frequency ranges.

In the frequency domain, input and output of a linear system are correlated by the transfer function H. In the case of random signal treatment the use of respective PSD-functions is more convenient, eq. (1).

$$\Phi_\varepsilon (Re,f) = |H(f)|^2 \, \Phi_p (Re,f) \qquad (1)$$

Φ_ε, Φ_p, - PSD functions of strain and pressure

Both, the input and output PSD-functions depend on coolant flow parameters (Reynolds number, Re) and the frequency, f. In our case the PSD function of pressure fluctuations Φ_p was used as input function and correlated to the PSD-function of strain, Φ_ε.
The integral RMS-value for a selected frequency range a - f - b is obtained from eq. (1) by integration

$$\left[\int_a^b \Phi_\varepsilon(Re,f)\,df\right]^{1/2} = \left/\int_a^b |H(f)|^2\,\Phi_p(Re,f)df\right/^{1/2} \qquad (2)$$

Applying the extended first theorem of the mean value, eq. (2) becomes

$$\left[\int_a^b \Phi_\varepsilon(Re,f)df\right]^{1/2} = |H(\mu)|\left[\int_a^b \Phi_p(Re,f)df\right]^{1/2} \qquad (3)$$

$$a \leq \mu \leq b;\ \Phi_p \geq 0 \text{ for } a \leq f \leq b$$

The "selective transfer function" $|H(\mu)|$ is then defined by eq. (4)

$$|H(\mu)| = \frac{\left[\int_a^b |H(f)|^2\,\Phi_p(Re,f)df\right]^{1/2}}{\left[\int_a^b \Phi_p(Re,f)df\right]^{1/2}} = F(Re) \qquad (4)$$

This function is generally real and positive in the frequency range considered. Introducing the strain and pressure coefficients [3,4], eq. (5) into eq. (3)

$$C_\varepsilon(Re) = \frac{\sqrt{\int_a^b \Phi_\varepsilon\,df}}{\bar{p}}\ ;\ C_p(Re) = \frac{\sqrt{\int_a^b \Phi_p\,df}}{\bar{p}} \qquad (5)$$

where $\bar{p}$ is the mean value of dynamic pressure, eq. (6),

$$\bar{p} = \frac{\rho \cdot \bar{v}^2}{2} \qquad (6)$$

one obtains eq. (7)

$$C_\varepsilon(Re) = F(Re)\ .\ C_p(Re). \qquad (7)$$

Using the simple empirical relationship between the pressure coefficient C_p and Reynolds number as given in eq. (8) [3,4]

$$C_p(Re) = C_1\,Re^{-C_2} + C_3 \qquad (8)$$

C_i - constants

the vibrational behaviour can be described by an empirical relationship of the form given in eq. (9)

$$C_\varepsilon(Re) = F(Re)\,(C_1\,Re^{-C_2} + C_3). \qquad (9)$$

Fig. 5 schematically illustrates characteristic shapes of the curves as defined by eq. (8) and (9) and as obtained experimentally. Whereas $C_p(Re)$ normally approximates a smooth constant value C_3 with increasing Reynolds number, $C_\varepsilon(Re)$ shows "resonances" (term proposed in analogy) which are interpreted as "resonant" excitation of normal modes. In other words, the transfer function, eq. (4), is not constant for the region of Reynolds number investigated.

A simple estimation of the upper and lower limit of $C_\varepsilon(Re)$ can be derived applying the following inequality relation, eq. (10)

$$m\,(C_1\,Re^{-C_2} + C_3) - C_\varepsilon - M\,(C_1 \cdot Re^{-C_2} + C_3) \qquad (10)$$

$$m = F(Re)_{min};\ M = F(Re)_{max}$$

$$a \leq f \leq b$$

and used to evaluate the feasibility of the tested structure with respect to vibrational behaviour.

5. Experimental results and interpretation

The vibrational behaviour of the tested subassembly is illustrated in fig. 6, where the so-called selective transfer functions are given as function of Reynolds number. The frequency ranges for which those functions have been calculated were chosen according to the calculated eigenfrequencies of characteristic structural parts (see fig. 3). The transfer functions obtained from the signals of two different strain gauges are similar to those expected from the symmetry of the subassembly and sensor arrangement.

In both cases there is a more or less definite resonance at medium Reynolds number for the selective transfer functions of the frequency range from C to 50 Hz. This resonance should, according to the calculations, be due either to strain gauge vibrations induced by periodic flow pulsations or to low frequency vibrations of the total pin bundle.

This transfer function increases again with higher Reynolds numbers most probably due to excitation of low frequency vibrations of the stiff wrapper caused by intense loop vibrations at high mass flow. The excitation functions of the next frequency interval (50 to 150 Hz, bundle and wrapper vibrations as calculated) show a similar dependence upon Reynolds number with the exception of any distinct resonance. The stronger excitation at lower Reynolds numbers could be interpreted as low frequency bundle vibrations, not as periodic flow fluctuations which should cause less vibration than in the low frequency region. The increase at higher Reynolds numbers can again be due to low frequency wrapper vibrations, but also due to low frequency bundle vibrations excited at higher mass flow.

The selective transfer functions for the higher frequency intervals chosen (150 to 600 Hz and 1.0 to 2.5 kHz) are somewhat different and similar to those theoretically expected when no distinct resonance is present. In the frequency region from 150 to 600 Hz the fuel pin vibrations should be predominant, which have been investigated by various authors [3,4,5,7] and no resonances in the vibration coefficients were reported. A similar behaviour can be expected for the vibrations of the total bundle which, according to the calculations (see fig. 3) would be predominant in the frequency region from 1.0 to 2.5 kHz.

6. Conclusions

The described arrangement of strain gauges using a minimum of sensors was tested successfully, apart from one early failure due to rupture. The experimental results are rather complex due to the vibrations of different characteristic structural parts which are sensed simultaneously. The proposed empirical approach to analysis and interpretation seems especially suitable for measurements in sodium with full-size subassemblies or other complex structures, when neither vibration measurements are the goal of the test, nor fundamental results are to be expected. This technique yields some additional insights into the physical interpretation of complex intra fuel assembly vibrations. The method of measurement and analysis first used in this test and therefore somewhat unexperienced, will be adopted for future tests and will certainly lead to further refinement.

List of symbols

a	lower limit of the frequency range
b	upper limit of the frequency range
C_ε	strain coefficient
C_p	pressure coefficient
C_i	empirical constants
f	frequency
F	selective transfer function
H	transfer function
m	minimum value of F
M	maximum value of F
$\overline{p}$	mean value of dynamic pressure
Re	Reynolds number
s	range of eigenfrequencies
$\overline{v}$	mean value of fluid velocity
ε	strain
Φ	power spectral density
Φ_ε	power spectral density of strain
Φ_p	power spectral density of pressure
μ	value of frequency within the range a,b
ρ	fluid density

References

[1] HESS, B., RUPPERT, E., STEHLE, H., VINZENS, K., "Studies to single subassembly flow monitoring with a complete 7 element array under sodium", Third Intern. Conf. on Structural Mechanics in Reactor Technology, London, Great Britain, September 1-5, 1974

[2] ZURMÜHL, R., "Matrizen", Springer, Berlin, 1961

[3] KADLEC, I., APPELT, K.D., "Flow-induced rod vibrations of fast reactor subassemblies", Nucl. Eng. Design 14, 136-150 (1970)

[4] HESS, B., BENEMANN, A., BROCKMANN, K., RELIC, M., "Investigations of coolant fluctuations within fast breeder fuel element bundle flow", Intern. Symp. on Vibration Problems in Industry, Keswick, English Lakes, April 10-12, 1973

[5] OHLMER, E., SCHWEMMLE, R., "Investigation on vibration behaviour and driving forces for fuel element models in parallel flow", Second Intern. Conf. on Structural Mechanics in Reactor Technology, Berlin, Germany, September 10-14, 1973

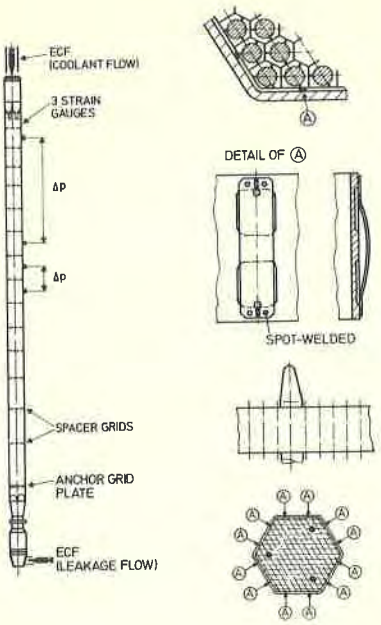

fig. 1 Schematic representation of the tested fuel subassembly, their instrumentation and the features of spacer grids

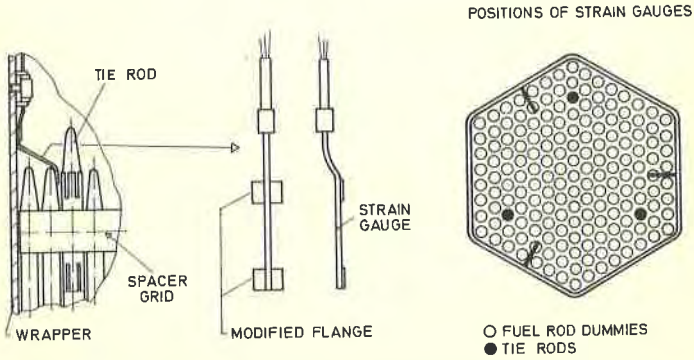

fig. 2 Schematic illustration of the experimental arrangement of especially deformed strain gauges

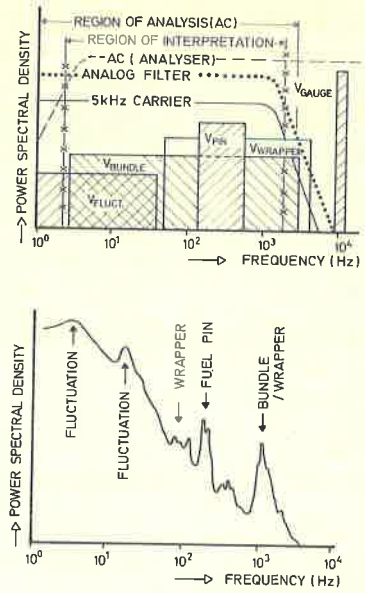

fig. 3 Schematic representation of a typical PSD-function of strain signals (below) and of calculated frequency ranges for vibrations of structural parts (above) where the frequency characteristics of the signal processing equipment are also schematically indicated

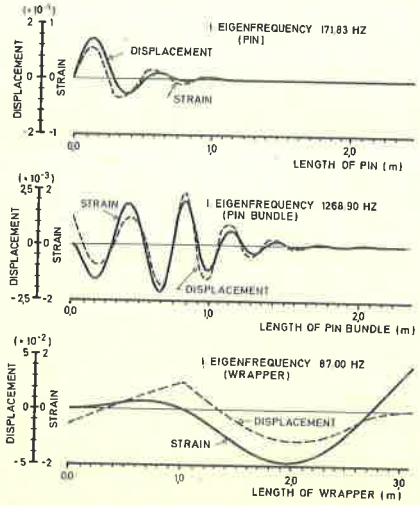

fig. 4 Calculated first modes of strain and displacement for a single fuel pin (free support), for the pin bundle (clamped) and for the wrapper tube (threefold clamped)

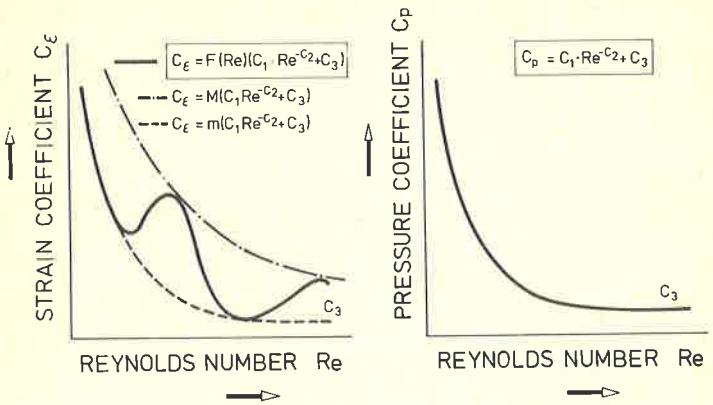

fig. 5 Schematic illustration of experimentally obtained strain coefficients $C_\varepsilon(Re)$, pressure coefficients $C_p(Re)$ and the illustration of minimum resp. maximum approximations, eq. (10)

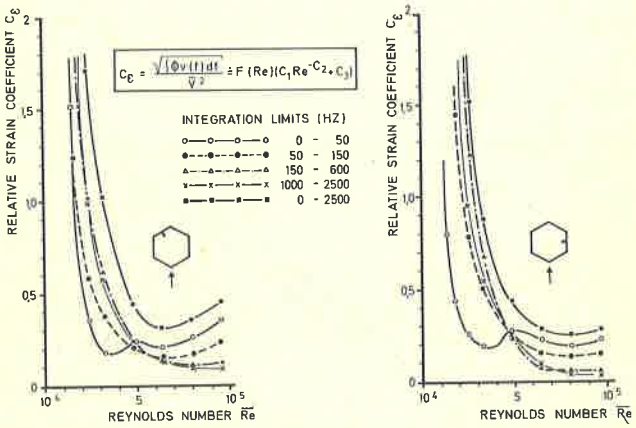

fig. 6 Selective transfer functions as obtained from the measurements at two different positions as indicated

C 2/9

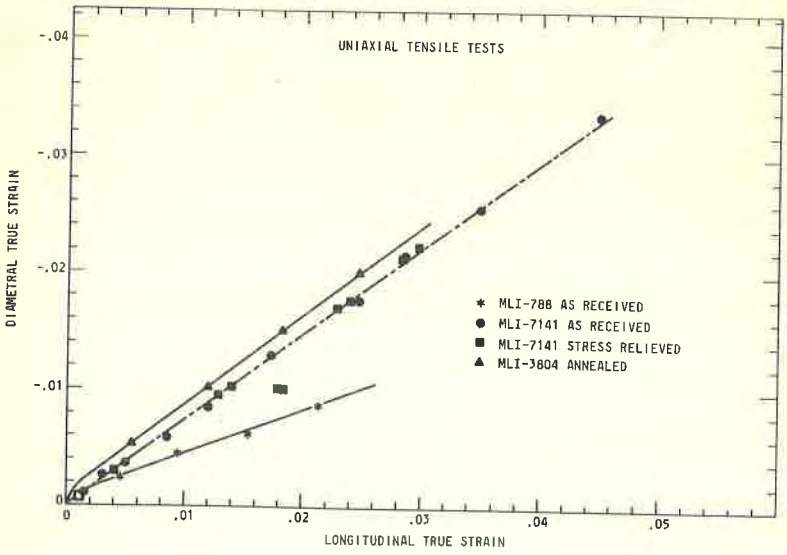

FIGURE 5 Diametral vs. Longitudinal true plastic strain for uniaxial tensile tests.

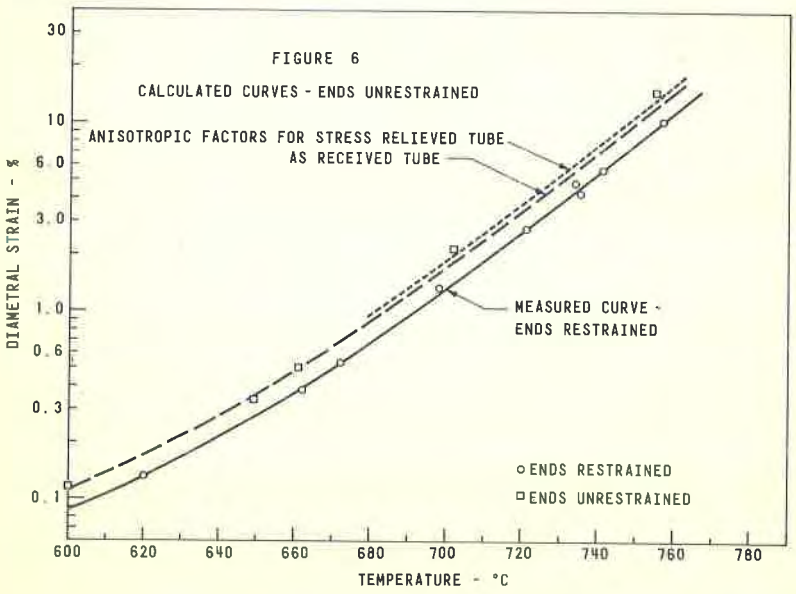

FIGURE 6 Comparison of measured and predicted diametral plastic strain for tubes with and without ends restrained.